U.S. Department of Veterans Affairs
Public Access Author manuscript
J Mol Cell Cardiol Plus. Author manuscript; available in PMC 2024 November 06.

Published in final edited form as:
J Mol Cell Cardiol Plus. 2024 September ; 9: . doi:10.1016/j.jmccpl.2024.100088.

Cardiac overexpression of a mitochondrial SUR2A splice variant impairs cardiac function and worsens myocardial ischemia reperfusion injury in female mice

Allison C. Wexler[a,b], **Holly Dooge**[a,b], **Sarah El-Meanawy**[a,b], **Elizabeth Santos**[a], **Timothy Hacker**[c], **Aditya Tewari**[a], **Francisco J. Alvarado**[a,c], **Mohun Ramratnam**[a,b,*]

[a]Division of Cardiovascular Medicine, Department of Medicine, University of Wisconsin School of Medicine and Public Health, Madison, WI 53705, USA

[b]Cardiology Section, Medical Service, William. S. Middleton Memorial Veterans Hospital, Madison, WI 53705, USA

[c]Cardiovascular Research Center, University of Wisconsin School of Medicine and Public Health, Madison, WI 53705, USA

Abstract

The small splice variant of the sulfonylurea receptor protein isoform 2 A (SUR2A-55) targets mitochondria and enhances mitoK_{ATP} activity. In male mice the overexpression of this protein promotes cardioprotection, reducing myocardial injury after an ischemic insult. However, it is unclear what impact SUR2A-55 overexpression has on the female myocardium. To investigate the impact of SU2R2A-55 on the female heart, mice with cardiac specific transgenic overexpression of SUR2A-55 ($TG^{SUR2A-55}$) were examined by resting echocardiography and histopathology. In addition, hearts were subjected to ischemia reperfusion (IR) injury. Female $TG^{SUR2A-55}$ mice had resting LV dysfunction and worse hemodynamic recovery with increased infarct size after IR injury. RNA-seq analysis found 227 differential expressed genes between WT and $TG^{SUR2A-55}$ female mouse hearts that were enriched in pathways of cellular metabolism. This was in direct contrast to male mice that had only four differentially expressed genes. Female $TG^{SUR2A-55}$ mice compared to female WT mice had reduced cardiomyocyte mitochondrial membrane potential without a change in electron transport chain protein expression. In addition, isolated mitochondria

*Corresponding author at: University of Wisconsin, Department of Medicine, 600 Highland Ave., Madison, WI 53792-0001, USA. mramrat@medicine.wisc.edu (M. Ramratnam).

Declaration of competing interest

The authors declare that they have no known competing financial interests or personal relationships that could have appeared to influence the work reported in this paper.

CRediT authorship contribution statement

Allison C. Wexler: Writing – review & editing, Writing – original draft, Visualization, Validation, Methodology, Investigation, Formal analysis, Data curation. **Holly Dooge:** Writing – original draft, Visualization, Formal analysis, Data curation. **Sarah El-Meanawy:** Formal analysis, Data curation. **Elizabeth Santos:** Writing – original draft, Formal analysis, Data curation. **Timothy Hacker:** Conceptualization. **Aditya Tewari:** Formal analysis, Data curation. **Francisco J. Alvarado:** Methodology. **Mohun Ramratnam:** Writing – review & editing, Writing – original draft, Visualization, Supervision, Software, Resources, Project administration, Methodology, Investigation, Funding acquisition, Conceptualization.

Appendix A. Supplementary data

Supplementary data to this article can be found online at https://doi.org/10.1016/j.jmccpl.2024.100088.

from female $TG^{SUR2A-55}$ hearts displayed reduced sensitivity to ATP and diazoxide suggestive of increased mitoK_{ATP} activity. In conclusion, our data suggests that female $TG^{SUR2A-55}$ mice are unable to tolerate a more active mitoK_{ATP} channel leading to LV dysfunction and worse response to IR injury. This is in direct contrast to our prior report showing cardioprotection in male mice overexpressing SUR2A-55 in heart. Future research directed at examining the expression and activity of mitoK_{ATP} subunits according to sex may elucidate different treatments for male and female patients.

Keywords

ATP sensitive potassium channels; Sulfonylurea receptors; Myocardial ischemia reperfusion injury; Cardiac metabolism; Sex differences

1. Introduction

Ischemic heart disease is a major burden to society and remains the leading cause of death for men and women [1]. In the United States, a heart attack occurs every 40 s [2] underscoring the significant impact of myocardial infarction (MI) in everyday life. While the treatment of acute MI has improved with the advent of reperfusion therapies, the detrimental effects of ischemia reperfusion (IR) injury persist with no current clinical remedies. There exist several potential targets described in the literature to treat IR injury. The mitochondrial ATP sensitive potassium channel (mitoK_{ATP}) is a notable channel that promotes cardioprotecton when activated [3,4]. The channel is composed of a mitochondrial K+ pore [5–7] and regulatory subunits [5,8,9]. Activation of mitoK_{ATP} prevents IR injury and mediates mitochondrial swelling, reactive oxygen species generation, ATP production and Ca^{2+} handling [3,10–12].

In 2009, Ye et al. described a small splice variant of the sulfonylurea receptor isoform 2 A (SUR2A-55) which localizes to mitochondria and enhances mitoK_{ATP} activity [13]. We observed that overexpression of the SUR2A-55 variant in male mice leads to cardioprotection via increased mitoK_{ATP} activity and altered glucose metabolism [8,14]. However, it is unclear if this observed effect exists in female mice. Multiple studies have reported different outcomes from human heart disease and animal models of heart disease based on sex. [15–19]. Premenopausal women fare better than men after an MI, including reduced ischemia-perfusion (IR) injury and improved chances of long-term survival [15]. While the precise mechanisms responsible for the relative cardioprotection observed in females versus males is still unclear, there is considerable evidence that downstream signaling after estrogen receptor activation lies at the center of female related cardioprotection [16,20]. One potential downstream signal of the estrogen receptor is K_{ATP} channels [21]. K_{ATP} channels are known to have increased expression in female hearts compared to male hearts due to an increase in SUR2A expression [22,23].

Consideration of sex differences in the treatment of ischemic heart disease is uncommon in part due to historical under-representation of women in research, both clinically and in animals [20]. Therefore, deciphering the nuances of sex differences in ischemic heart disease will enhance our understanding of the mechanisms of cardiovascular disease and will lead to

the development and improvement of cardioprotective therapies. In this study, we explored the impact of SUR2A-55 overexpression in female mouse hearts on cardiac structure and function, and the resulting response to acute ischemic injury.

2. Material and methods

2.1. Experimental animal

All animal procedures and experiments were performed with approval from the Institutional Animal Care and Use Committee at the University of Wisconsin and comply with the National Research Council's Guide for the Care and Use of Laboratory Animals. For each experiment, four to nine $TG^{SUR2A–55}$ or WT littermate control mice aged 9–15 weeks were used. For each figure the sample size is provided. $TG^{SUR2A–55}$ mice were previously generated by overexpression of a SUR2A-55 construct by the α-myosin heavy chain promoter [8] on a C57BL/6 J strain background.

2.2. Quantitative PCR

Total RNA was extracted from male and female mouse ventricular tissue using TRIzol reagent (Invitrogen ThermoFisher, Waltham, MA) according to the manufacturer's instructions. RNA concentration and purity were determined using NanoDrop One Microvolume UV–Vis Spectrophotometer (Invitrogen ThermoFisher, Waltham, MA). First strand cDNA was synthesized from 500 ng of total RNA using Super-Script IV VILO Master Mix (Invitrogen ThermoFisher, Waltham, MA) and the following conditions: 25 °C for 10 min, followed by 50 °C for 10 min and 85 °C for 5 min. The quantitative real-time PCR (qPCR) reaction was performed using a 1:5 dilution of cDNA in a total of 20 uL with 10 uL PowerTrack SYBR Green Master Mix (Invitrogen ThermoFisher, Waltham, MA) and a final concentration of 400 nM forward primer and 400 nM reverse primer. Reactions containing no-RT and NTC controls were included for all experiments. Each cDNA sample was analyzed for gene expression by qPCR using the BioRad CFX 96 Real-Time PCR Detection System. Amplification data were analyzed using the delta-delta Ct method. The conditions of qPCR for all primer/probe sets were as follows: an initial denaturation at 95 °C for 2 min followed by 40 cycles at 95 °C for 15 s and 60 °C for 1 min. Reactions were completed with a dissociation step of 95 °C for 15 s at a ramp rate of 1.6C/S, then 60 °C for 1 min at a ramp rate of 1.6C/s, and lastly 95 °C for 15 s at a ramp rate of 0.08C/s. Oligonucleotide primers were designed using published sequence data from GenBank with the aid of PrimeQuest Design Tool (Integrated DNA Technologies, Coralville, IA). The primer sequences used are shown in Supplementary table 1. RNA expression was normalized to the levels of GAPDH RNA as the reference gene.

2.3. Cardiac structure and function by echocardiography

Transthoracic echocardiography was performed on eight WT and nine $TG^{SUR2A-55}$ female mice (10.3 ± 0.5 vs 9.8 ± 0.2 weeks of age respectively; $p = 0.18$) after sedation with 3 % and maintenance with 1.5 % isoflurane using a VisualSonics Vevo 3100 machine with a 30-MHz transducer [8]. Left ventricular end diastolic (LVID;d), left ventricular end systolic (LVID;s), anterior wall thickness in diastole (LVAW; d) and posterior wall thickness in diastole (LVPW;d) were obtained from M-mode tracings. LV fractional shortening was

calculated with the following equation;(LVEDD–LVESD)/LVEDD×100 %. LV ejection fraction was obtained from B-mode echocardiography.

2.4. Gross pathology

Five WT and six $TG^{SUR2A\text{-}55}$ female mice aged 10–14 weeks were sedated with 3 % isoflurane and weighed before being euthanized by cervical dislocation. The heart and lungs were quickly excised, blotted dry, cleaned of excess tissue, and weighed to obtain heart to body weight and lung to body weight ratios.

2.5. Histopathological analysis

11-week-old WT and $TG^{SUR2A\text{-}55}$ female mouse hearts were sectioned and stained with hematoxylin and eosin to assess myofiber architecture, Masson's trichrome to assess interstitial fibrosis, and picrosirius red to appraise collagen networks qualitatively. Images were taken using an EVOS microscope under 5× magnification with light microscopy.

2.6. Langendorff-perfused hearts

Isolated mouse hearts were perfused according to the Langendorff technique at constant pressure as previously described [8]. Female mice, ages 9–15 weeks, were euthanized by cervical dislocation, then hearts were quickly excised from the chest. The aorta was cannulated with a 22-gauge metal cannula, then secured with silk suture and hung on an isolated perfused heart system for small rodents (Harvard Apparatus, Holliston, MA). Hearts were perfused at 37 °C at constant pressure of 80 mmHg with a modified Krebs-Henseleit Buffer (118 mM NaCl, 22 mM NaHCO3, 4.7 mM KCl, 1.2 mM MgSO4, 1.1 mM KH2PO4, 2.5 mM CaCl2, 5 mM Glucose, 2 mM Sodium Pyruvate). During initial perfusion, the left atrium was excised, and a pressure sensing balloon was inserted into the left ventricle. Global ischemia was induced by turning off flow to the isolated mouse heart. Hearts were subjected to 20 min of perfusion at baseline, followed by 45 min of global ischemia then 60 min of reperfusion. IR experiments were excluded from analysis if 1.) the aortic block pressure or left ventricular developed pressure fell below 60 cm H_2O during the initial 20-min perfusion, 2.) there was observed abnormally slow, fast, or arrhythmic beating, or 3.) there was an observed abnormal flow rate out of the heart during initial perfusion. After the IR injury protocol, hearts were removed from the Langendorff apparatus and arrested in diastole with 5 min of perfusion with 30 mM KCl in PBS. Hearts were then stained at 37 °C with 1 % TTC in phosphate buffer (23.1 mM NaH2PO4, 76.9 mM Na2HPO4, 29.9 mM 2,3,5-Triphenyltetrazolium chloride TTC), frozen and cut into 1 mM transverse slices. Sections were then imaged under light microscopy and photographed. Infarct size was determined through color threshold calculations in ImageJ (white pixels/pixels at risk).

2.7. RNA-Seq and bioinformatics

The hearts of four male and four female WT and $TG^{SUR2A\text{-}55}$ mice were collected for transcriptome analysis by RNA-seq. Mice were deeply anesthetized with 5 % isoflurane and hearts were harvested immediately after sacrifice of the mouse, washed in PBS, and flash frozen in liquid nitrogen. 1/3 of the apical mouse heart was used for RNA extraction. RNA extraction, quality control, library preparation, sequencing, alignment,

and differential gene expression analysis were conducted by the University of Wisconsin Biotechnology core center. Total RNA was extracted from frozen tissue samples using Qiagen RNeasy Plus Universal Mini Kit (Qiagen, Hilden, Germany) with an on-column DNA digest. The quantity and quality of extracted RNA was accessed with a NanoDrop One Spectrophotometer (Thermo-Fisher Scientific, Waltham, MA).

Samples that met the Illumina sample input guidelines were prepared according the TruSeq® Stranded mRNA Sample Preparation Guide (Rev. E) using the Illumina® TruSeq® Stranded mRNA Sample Preparation kit (Illumina Inc., San Diego, California, USA). For each library preparation, mRNA was purified from 1000 ng total RNA using poly-T oligo-attached magnetic beads. Subsequently, each poly-A enriched sample was fragmented using divalent cations under elevated temperature. The mRNA fragments were converted to double-stranded cDNA (ds-cDNA) using Superscript II (Invitrogen, Carlsbad, California, USA), RNaseH and DNA Pol I, primed by random primers. The ds cDNA was purified with AMPure XP beads (Agencourt, Beckman Coulter). The cDNA products were incubated with Klenow DNA Polymerase to add an 'A' base (Adenine) to the 3' end of the blunt DNA fragments. DNA fragments were ligated to Illumina unique dual adapters, which have a single 'T' base (Thymine) overhang at their 3'end. The adapter-ligated DNA products were purified with AMPure XP beads. Adapter ligated DNA was amplified in a Linker Mediated PCR reaction (LM-PCR) for 10 cycles using PhusionTM DNA Polymerase and Illumina's PE genomic DNA primer set followed by purification with AMPure XP beads. Finally, the quality and quantity of the finished libraries were assessed using an Agilent DNA1000 chip (Agilent Technologies, Inc., Santa Clara, CA, USA) and Qubit® dsDNA HS Assay Kit (Invitrogen, Carlsbad, California, USA), respectively. Libraries were standardized to 2 nM. Paired-end 2x150bp sequencing was performed, using standard SBS chemistry on an Illumina NovaSeq6000 sequencer. Images were analyzed using bcl2fastq v2.20.0.422. The trimming software skewer [24] was used to preprocess raw fastq files. After adapter trimming, the University of Wisconsin Bioinformatics Resource Center RNA-Seq pipeline computes eight QC statistics before further analysis. Low abundance genes defined as those with an average read count below a threshold of 1.0 in two or more samples were then filtered out of the dataset. The RNA-seq data was then normalized by the method of trimmed mean of M-values (TMM) [25]. Alignment was performed by using STAR (Spliced Transcripts Alignment to a Reference) against *Mus musculus* [26]. Mapped paired-end reads for both genes and transcripts (isoforms) are counted in each sample using RSEM [27]. Analysis of differentially expressed genes was performed using the edgeR package [25].

Analysis of significantly differentially expressed genes (DEGs) was completed in RStudio 2021.09.1. Log2 fold changes versus adjusted *P* value on a negative log 10 scale were plotted for each differentially expressed gene (DEG) in a volcano plot. The heat map depicts the top 50 DEGs with an FDR corrected *p*-value of <0.05. DEGS were then subject to Gene ontology enrichment analysis.

2.8. Isolation of mitochondria from mouse hearts

Mitochondria from murine ventricular cardiac tissue were isolated by homogenization and differential centrifugation as previously described [14]. Hearts were quickly excised and

placed in ice-cold isolation buffer (50 mM sucrose, 200 mM mannitol, 5 mM KH2PO4, 1 mM EGTA, and 5 mM 3-(N-morpholino)propanesulfonic acid). Atrial tissue was removed, and the remaining ventricles were minced and digested for 10 min with 0.1 mg/mL of trypsin. Mitochondrial isolates were treated with a protease inhibitor during the isolation process (Pierce Protease Inhibitor, ThermoFisher Scientific). Protein concentrations were determined using the Bradford method.

2.9. Western Blot analysis

Western blots were performed by suspending 30μg of homogenate tissue in Laemmli buffer and separating proteins through SDS-PAGE in 4–20 % TGX precast gels (Bio-Rad). Transfer to PVDF membranes was completed using the iBlot2 Dry Blotting system, after which antibody incubation was carried out in the iBind Flex Western Device (Thermo-Fisher). Membranes were probed with the following primary antibodies: (total Oxphos, 1:250, ab110413, Abcam; HSP60, 1:1000, ab45134, Abcam). The secondary antibody required by all blots was Goat Anti-Rabbit IgG H&L HRP (1:2000, ab205718, Abcam). SuperSignal ECL reagent (Thermo) was used to develop membranes which were subsequently imaged with a ChemiDoc MP apparatus (Bio-Rad). Band intensity was quantified in ImageLab software (Bio-Rad).

2.10. Measurement of Membrane Potential in Isolated Cardiomyocytes

Two cell isolations were performed nearly simultaneously, with one female WT and one female $TG^{SUR2A\text{-}55}$ used for each experimental run. Mice were dosed with an intraperitoneal injection of 200 units of heparin and returned to the carrier for 15 min before euthanasia by cervical dislocation. The heart was excised and dissected in a dish containing perfusion buffer (10 mM HEPES, 0.6 mM Na2HPO4, 113 mM NaCl, 4.7 mM KCl, 12 mM NaHCO3, 0.6 mM KH2PO4, 1.2 mM MgSO4-7H2O, 10 mM KHCO3, 30 mM Taurine, 5.55 mM Glucose, pH 7.4) and 2000 units of heparin. The aorta was cannulated with a 22 g metal cannula and secured with 6–0 silk. The cannula was then secured to a custom perfusion apparatus and perfused at 37 °C at a constant flow rate of 3–4 mL/min for 5 min. Hearts were then digested by a 6–10 min perfusion of buffer containing 25 μM CaCl2 and 2–3 mg Liberase TL.

Hearts were then removed from the cannula and placed in a dish of stopping buffer (18 mL perfusion buffer, 2 mL FBS, 12.5 μM CaCl2). The atria were removed and discarded, then the remaining ventricles were gently pipetted into a suspension. The cell suspension was pipetted through nylon mesh into a 15 mL tube and allowed to settle. The supernatant was discarded, and the cell pellet was resuspended in an additional 4 mL of stopping buffer. Calcium was slowly reintroduced to the cells in increments of 20 μl of 10 mM CaCl2, 20 μl of 10 mM CaCl2, 40 μl of 10 mM CaCl2, 12 μl of 100 mM CaCl2 and 20 μl of 100 mM CaCl2 for a final concentration of 1 mM, with 4 min of incubation at room temperature after each addition. Cells were allowed to sediment again, the supernatant was discarded, and the pellet was resuspended in 2 mL of Tyrode Mouse buffer (135 mM NaCl, 4 mM KCl, 1 mM MgCL2, 10 mM HEPES, 1.2 mM NaH2PO4-H2O, 10 mM Glucose, 1.8 mM CaCl2, pH 7.4).

Cell suspensions were plated on laminin-coated, glass bottom 30 mM dishes and incubated for one hour at room temperature. Plates were then treated with 2 nM TMRE and incubated for an additional 30 min at 37 °C, protected from light. One plate from each experimental group was treated with 1 uM FCCP in addition to TMRE. Plates were washed with Tyrode buffer before imaging under a Zeiss LSM800 confocal microscope at room temperature. Cells were located under 10× magnification with transmitted light, then imaged under 20× magnification with an excitation λex of 561 nm and emission λem from 565 to 700 nm. Cells were analyzed in image J. Each cell was encircled and the average florescence for each cell minus background was recorded representing resting mitochondrial membrane potential.

2.11. Mitochondrial membrane potential assessment in isolated cardiac mitochondria

Mitochondrial membrane potential (Δψm) was monitored spectrophotometrically as previously described [14]. Briefly, using rhodamine 123 (5 nM) and excitation λex of 503/510-nm and emission λem of 527/535-nm for coupled and uncoupled mitochondria respectively, 0.25 mg of mitochondria were added to a cuvette containing malate (5 mM), pyruvate (5 nM) and oligomycin (1 μg/mL). The ATP sensitivity of Δψm was assessed after the addition of 1000 μM of ATP to a cuvette containing no ATP. To assess the activity of mitoK_{ATP}, diazoxide (100 μM), was administered [24]. The ionophore carbonylcyanide-4-trifluoromethoxyphenylhydrazone (FCCP; 10 μM) was used to depolarize the Δψm at the end of each experiment. One μg of Phosphatidylinositol 4,5-bisphosphate (PIP2, Avanti, Birmingham, AL) was administered to prevent mitoK_{ATP} run down in isolated mitochondrial preparations in the cuvette prior to mitochondrial addition [28]. Differences between groups were assessed using absolute florescence (a.f.u.) changes after ATP administration.

2.12. Data analysis

Data are reported as mean ± standard deviation. Statistical analyses were performed using the R program 3.4.2 (R Foundation for Statistical Computing) and Microsoft Excel (Microsoft, Redmond, WA, USA) with a p value <0.05 considered significant. Shapiro–Wilk's test was used to assess normality. Comparisons between two groups were made using the two-tailed Student's t-test. Statistical differences between more than two groups were performed by two-way ANOVA.

3. Results

3.1. The overexpression of SUR2A-55 causes a cardiomyopathy in female mice

Both male and female $TG^{SUR2A-55}$ mice have increased expression of the *Abcc9* gene splice variant that encodes the small 55 kD SUR2A-55 protein compared to WT mice (Supplementary Fig. 1). In addition, $TG^{SUR2A-55}$ mice have no difference in the expression of the full-length *Abcc9* mRNA compared to WT mice. We also found no significant difference between the expression of *Abcc9* gene products between male and female $TG^{SUR2A-55}$ mice. We found no gross histologic differences between female WT and $TG^{SUR2A-55}$ mice with hematoxylin and eosin, mason trichrome or picrosirius red staining (Fig. 1 A). In addition, assessments of gross pathology (Fig. 1C and D) did not show any difference in heart weight to body weight and lung weight to body weight ratios.

Echocardiographic analysis indicated that $TG^{SUR2A-55}$ mice had a significantly larger left ventricular internal diameter at end systole (Fig. 1F). Wall thickness was similar in both mouse groups. Fractional shortening and ejection fraction measurements were significantly lower in $TG^{SUR2A-55}$ mice compared to WT mice (Fig. 1G) without a significant change in heart rate.

3.2. $TG^{SUR2A-55}$ female mice have worse response to ex-vivo IR injury

Isolated hearts from female WT and $TG^{SUR2A-55}$ mice were subjected to 45 min of no flow ischemia and then 60 min of reperfusion. $TG^{SUR2A-55}$ female mice had reduced +dp/dt and −dp/dt compared to WT female mice during baseline *ex vivo* perfusion (Table 1). The spontaneous heart rate, left ventricular developed pressure, and double product were not statistically significant between mouse groups during baseline *ex vivo* perfusion (Table 1). During IR injury, $TG^{SUR2A-55}$ had diminished left ventricular developed pressure (LVDP) and double product (DP) compared to WT mice (Fig. 2B and C). $TG^{SUR2A-55}$ mice also had decreased +dp/dt and −dp/dt compared to WT mice during reperfusion (Fig. 2D and E). Representative heart sections stained with 1 % TTC from $TG^{SUR2A-55}$ and WT mice after IR injury showed significantly increased myocardial infarction in $TG^{SUR2A-55}$ compared to WT mice (Fig. 2A).

3.3. RNA-seq analysis reveals alterations in mitochondrial function at rest in female but not male $TG^{SUR2A-55}$ mice compared to WT mice

To elucidate the mechanisms by which the overexpression of SUR2A-55 exerts its detrimental effect on female mouse hearts, we examined gene expression by RNA-seq. Using a false discovery rate (FDE) of <0.05 and log2 fold change >0.58 we identified 227 deferentially expressed genes (DEGs) between female $TG^{SUR2A-55}$ vs. WT littermate control mice. (Fig. 3 and https://www.ncbi.nlm.nih.gov/geo/query/acc.cgi?acc=GSE245038 with GEO series accession number GSE245038). The *Abcc9* gene product was greatly increased compared to WT mice hearts due to the overexpression model and removed from fig. 3 to highlight alternative genes and pathways. The original data including *Abcc9* expression is provided in supplementary fig. 2 for both male and female $TG^{SUR2A-55}$ vs WT mice. In direct contrast to female mice, there were few differences in DGEs between WT and $TG^{SUR2A-55}$ male mice (https://www.ncbi.nlm.nih.gov/geo/query/acc.cgi?acc=GSE245038 with GEO series accession number GSE245038). This is congruent with our prior work showing no differences in baseline cardiac function or pathology between WT and $TG^{SUR2A-55}$ male mice [8].

The top 50 differentially expressed genes are represented in Fig. 3B and include upregulation of the metabolic and mitochondrial genes; *Por* (P450 (cytochrome) oxidoreductase), *Ndufb4c* (NADH:ubiquinone oxidoreductase subunit B4C), *Ndufa2* (NADH:ubiquinone oxidoreductase subunit A2), *Ndufb7*(NADH:ubiquinone oxidoreductase subunit B7), *Cox8b* (cytochrome *c* oxidase subunit 8B), *Cox6a2* (cytochrome *c* oxidase subunit 6A2), *bckdha* (branched chain ketoacid dehydrogenase E1, *Uqcr11* (ubiquinol-cytochrome *c* reductase complex III subunit XI), *Ndufa7* (NADH:Ubiquinone Oxidoreductase Subunit A7), *Acads* (acyl-Coenzyme A dehydrogenase short chain). Interestingly, multiple subunits of mitochondrial ETC complex I were affected by

SUR2A-55 overexpression in the female heart. We then obtained the top 20 Gene Ontology (GO) terms from the enrichment analysis of these DEGs (Fig. 3C) and performed a network analysis (Fig. 3D). We found significant enrichment of genes related to oxidative phosphorylation, aerobic respiration, cellular respiration, and the mitochondrial electron transport chain and other metabolic pathways. This suggested a role of SUR2A-55 in cardiac metabolism and energy production and potential effects of SUR2A on mitochondrial ETC function. Notably we did not see any changes in gene expression related to known ATP sensitive mitochondrial or sarcolemmal potassium channel pore expression.

3.4. Female $TG^{SUR2A-55}$ mice have reduced mitochondrial membrane potential ($\Delta\psi m$) at baseline

Since our gene expression analysis suggested changes at the mitochondrial level and ETC complex expression, we assessed $\Delta\psi m$ and selective protein expression of the ETC enzymes. We found that $TG^{SUR2A-55}$ female mice cardiomyocytes have a small but reduced resting $\Delta\psi m$. However, this was not accompanied by any changes in the ETC proteins we assessed (Fig. 4). In addition, we previously found that there were no changes in the protein expression levels of $mitoK_{ATP}$ pore forming subunits, CCDC51 and ROMK, between $TG^{SUR2A-55}$ and WT mouse hearts among either gender [14].

3.5. The cardiac $\Delta\psi m$ from female $TG^{SUR2A-55}$ mice are less sensitive to ATP and diazoxide compared to female WT mice

To assess the function of $mitoK_{ATP}$, we observed the response of $\Delta\psi m$ to ATP and the $mitoK_{ATP}$ opener, diazoxide, in isolated heart mitochondria from female $TG^{SUR2A-55}$ and WT mice (Fig. 5). The sensitivity of $\Delta\psi m$ to ATP was diminished in $TG^{SUR2A-55}$ mitochondria compared to WT mitochondria. In addition, diazoxide decreased the $\Delta\psi m$ in WT mitochondria more than the $\Delta\psi m$ of $TG^{SUR2A-55}$ mitochondria. These results are similar to our previous observations in male $TG^{SUR2A-55}$ [8]. However, while we found that this mitochondrial phenotype, suggestive of a more active $mitoK_{ATP}$ channel, produced cardioprotection in male mice, the opposite is observed in female $TG^{SUR2A-55}$ compared to WT female mice.

4. Discussion

In this study we found that cardiac specific overexpression of SUR2A-55 in female mice leads to left ventricular dysfunction and intolerance to IR injury compared to WT female mice. RNA-seq analysis of whole hearts revealed changes in gene expression related to oxidative phosphorylation, aerobic respiration, cellular respiration, and the mitochondrial electron transport chain among other metabolic pathways. While we found a small but statistically significant reduction in mitochondrial membrane potential, this was not accompanied by changes in ETC protein complex expression. However, we did find the mitochondrial membrane potential to be less responsive to ATP and diazoxide in $TG^{SUR2A-55}$ compared to WT female mice supporting a more active $mitoK_{ATP}$ channel. Our results contrast our prior findings showing cardioprotection in male mice overexpressing SUR2A-55 in heart. While the male mice data is historical in nature, our current findings are interesting and add to the observed sex differences between male and female hearts

after IR injury. In addition, our data underscores the importance of SUR2A-55 in cardiac metabolism.

Ye et al. originally described the SUR2A-55 splice variant of *Abcc9* in 2009 [13]. The investigators sought to determine why male mice with SUR2A knockout by deleting exon 14–18 surprising leads to a cardioprotective phenotype [29]. Mice with knockout of exon 14–18 in the *Abcc9* gene were found to still harbor a short splice variant of SUR2A named SUR2A-55 [13]. Male mice with exon 14–18 deletion not only demonstrated cardioprotection after IR Injury but also displayed favorable mitochondrial bioenergetics and heighted mitoK_{ATP} activity [30]. In addition, heterologous experiments with SUR2A-55 and K_{ATP} channel pore subunits found a channel that is more active and less responsive to pharmacology and inhibition from ATP [31]. These data suggested that SUR2A-55 may be a regulatory subunit for mitoK_{ATP}. Next, the examination of male mice with cardiac specific SUR2A-55 overexpression found no differences in cardiac structure or function at baseline compared to male WT mice. In contrast, we found that female $TG^{SUR2A\text{-}55}$ mice exhibited LV dysfunction at baseline compared to female WT mice. Additionally, while we previously found that male $TG^{SUR2A\text{-}55}$ mice compared to WT male mice displayed cardioprotection after IR injury [8], we found that female $TG^{SUR2A\text{-}55}$ mice demonstrated worse hemodynamic recovery and infarct size after IR injury compared to female WT mice. This finding is similar to a prior investigation in female mice with SUR2 knockout showing baseline LV dysfunction and worse response to IR injury [21]. We also found that female $TG^{SUR2A\text{-}55}$ mice had a more depolarized resting mitochondrial membrane potential with reduced sensitivity to ATP and diazoxide compared to WT controls, suggesting increased mitoK_{ATP} activity. In addition, while there were 227 differentially expressed genes between female WT and female $TG^{SUR2A\text{-}55}$ mice, there were only four differentially expressed genes between male WT and male $TG^{SUR2A\text{-}55}$ mice highlighting the impact of SUR2A-55 overexpression by sex.

One hypothesis to explain our observed findings in the context of our prior work in male mice may be the potential difference in the baseline activity of cardiac mitoK_{ATP} according to sex. Transgenic overexpression of SUR2A-55 in heart could confer different effects on cardiovascular physiology by sex. Our RNA-seq data provides support for a role of SUR2A-55 in regulating baseline metabolism in female mice as multiple genes related to mitochondrial function were altered compared to male mice hearts. While limited data exist examining the differences in mitoK_{ATP} activity by sex, some groups have looked at the differences in sarcolemmal K_{ATP} (sacrK_{ATP}) activity by sex. Prior studies found increased sacrK_{ATP} activity in female compared to male counterparts [22,23]. Activation of sacrK_{ATP} hyperpolarizes the cell - shortening the action potential, reducing Ca2+ entry, and reducing contractility. While this is a protective effect in cases of ischemia as it preserves ATP, excessive activity of sacrK_{ATP} is linked to heart failure [32] Interestingly, one report studying the long term effects of diazoxide administration on mouse neurologic behavior found difference in female mice behavior with increased doses of diazoxide. This contrasts with male mice, who did not display any dose response effect or differences compared to vehicle treated male mice [33]. Another report supports a connection between estrogen and K_{ATP}. Gao et al. found that sacrK_{ATP} is a downstream regulatory target of estrogen and plays a critical role in the mechanistic pathway of female stress signaling [21]. It may be that

K_{ATP} activity is a “double-edged sword:” too much activity at baseline limits proper cardiac performance, but insufficient activity under ischemic conditions prevents cardioprotection [32]. While females have increased sacrK_{ATP} activity [34] possibly through increased SUR2 expression, the expressions levels and activity of mitoK_{ATP} according to sex is less clear. It is also unclear if estrogen plays a significant role in the expression and function of mitoK_{ATP} components. This is specially made challenging by a lack of a robust assay for mitoK_{ATP} [35] and multiple candidates for the mitoK_{ATP} potassium pore [5,7,36]. However, given the heightened sarcK_{ATP} activity, WT females may have a heighted mitoK_{ATP} activity which results in baseline cardioprotection observed in many IR injury related papers. In addition, the overexpression of SUR2A-55 may increase the mitoK_{ATP} activity in females causing a tip in the balance from cardioprotection to dysfunction. Further research assessing mitoK_{ATP} activity and current mitoK_{ATP} subunit expression by sex would shed light on whether this hypothesis holds true and is planned for future studies.

Though our study showed the effect of SUR2A-55 overexpression on female cardiac structure and function, certain limitations are present. There is variation in our IR data particularity in our transgenic female mouse line. This may be due to different expression levels of SUR2A-55 between individual mice. In addition, we assessed cardiac injury in an *ex vivo* isolated heart model instead of an *in vivo* model, so there is imperfect translation to whole organisms. Also, we did not include a sham-operated control in our IR experiments. Since there is a baseline abnormal cardiac phenotype in $TG^{SUR2A-55}$ female mice, future *in vivo* IR experiments using a sham operative arm may be helpful in discerning the effect of this baseline dysfunction on IR injury. Additionally, while there were no changes in the methods of *ex vivo* IR experiments between our prior study of male mice and the current study, the two data sets may not be an ideal comparison due to the male mice dataset being procured at a different time. Furthermore, it is challenging to support hypothesis regarding SUR2A-55 influence on mitoK_{ATP} until the K+ pore binding partner for SUR2A-55 is identified. Prior research has suggested that ROMK, CCDC51, and ATP synthase are all possibilities [36]. We recently found that SUR2A-55 can regulate ROMK activity in cardiomyocytes [14]. In addition, a functional relationship between ROMK and SUR2B has been found in the kidney [37]. Therefore, future research identifying the relevant components of a SUR2A-55 based mitochondrial K+ channel with a focus on ROMK is needed. In addition, SUR2A-55 may be working via alternative mechanisms other than mitoK_{ATP}. Our RNA-seq data used whole heart samples and therefore it is plausible that other cardiac cell types (i.e. fibroblasts or vascular cells) may be impacted by the cardiomyocyte overexpression of SUR2A-55. RNA-seq data pointed to expression changes in the subunit of complex I in the ETC. While we did not find protein changes in ETC with the assay used, the protein expression of subunits directly linked to our RNA-seq data could be examined.

5. Conclusion

In this study, female mice with cardiac specific overexpression of SUR2A-55 have cardiac dysfunction and fair worse after IR injury compared to WT female mice while cardiac mitochondria display membrane depolarization with reduced sensitivity to ATP and diazoxide, suggesting a more active mitoK_{ATP} channel. This is contrast to our prior

report showing that transgenic male mice with SUR2A-55 cardiac overexpression far better compared to male WT controls. Gene expression analysis among our cohorts of female mice found significant changes in genes related to metabolism supporting prior work that SUR2A-55 regulates mitochondrial bioenergetics. Our work continues to support a role for SUR2A-55 in cardioprotection but adds new insight as female mice, unlike our prior work in male mice, do not tolerate SUR2A-55 overexpression. Future therapies targeting mitoK_{ATP} subunits will need to consider sex differences.

Supplementary Material

Refer to Web version on PubMed Central for supplementary material.

Acknowledgements

We would like to thank the University of Wisconsin - Atherosclerosis Imaging Research Program for murine echocardiography and analysis, the University of Wisconsin – Madison Biotechnology Center Gene Expression Center (Research Resource Identifier – RRID:SCR_017757) for RNA sequencing and library preparation and the University of Wisconsin-Madison Biotechnology Center Bioinformatics Core Facility (Research Resource Identifier – RRID:SCR_017799) for analysis services. BioRender was used to create the graphical abstract.

Funding

This research was supported in part by UL1TR002373 from NIH/NCATS (M.R.), Career Development Award IK2 BX004614 (M.R.) from the United States (U.S.) Department of Veterans Affairs Biomedical Laboratory Research and Development Service and University of Wisconsin Department of Medicine Pilot funding (M.R).

Abbreviations

mitoK_{ATP}	mitochondrial ATP sensitive potassium channel
SUR2A	sulfonylurea receptor isoform 2 A
SUR2A- 55	small 55 kDa splice variant of the sulfonylurea receptor isoform 2 A
IR	ischemia reperfusion
K_{ATP}	ATP sensitive potassium channel
sarcK_{ATP}	sarcolemmal ATP sensitive potassium channel

References

[1]. Cardiovascular diseases (CVDs) are the leading cause of death globally. Available from: https://www.who.int/health-topics/cardiovascular-diseases#tab=tab_1; 2021.

[2]. Tsao CW, et al. Heart disease and stroke Statistics-2023 update: a report from the American Heart Association. Circulation 2023;147(8):e93–621. 10.1161/CIR.0000000000001123. [PubMed: 36695182]

[3]. Ardehali H, O'Rourke B. Mitochondrial K(ATP) channels in cell survival and death. J Mol Cell Cardiol 2005;39(1):7–16. 10.1016/j.yjmcc.2004.12.003. [PubMed: 15978901]

[4]. O'Rourke B Evidence for mitochondrial K+ channels and their role in cardioprotection. Circ Res 2004;94(4):420–32. 10.1161/01.RES.0000117583.66950.43. [PubMed: 15001541]

[5]. Paggio A, et al. Identification of an ATP-sensitive potassium channel in mitochondria. Nature 2019;572(7771):609–13. 10.1038/s41586-019-1498-3. [PubMed: 31435016]

[6]. Foster DB, et al. Mitochondrial ROMK channel is a molecular component of mitoK (ATP). Circ Res 2012;111(4):446–54. 10.1161/CIRCRESAHA.112.266445. [PubMed: 22811560]

[7]. Juhaszova M, et al. ATP synthase K(+)- and H(+)-fluxes drive ATP synthesis and enable mitochondrial K(+)-"uniporter" function: I. Characterization of ion fluxes. Function (Oxf) 2022;3(2):zqab065. 10.1093/function/zqab065. [PubMed: 35229078]

[8]. Ramratnam M, et al. Transgenic overexpression of the SUR2A-55 splice variant in mouse heart reduces infract size and promotes protective mitochondrial function. Heliyon 2018;4(7):e00677. 10.1016/j.heliyon.2018.e00677. [PubMed: 29998196]

[9]. Ardehali H, et al. Multiprotein complex containing succinate dehydrogenase confers mitochondrial ATP-sensitive K+ channel activity. Proc Natl Acad Sci USA 2004;101(32):11880–5. 10.1073/pnas.0401703101. [PubMed: 15284438]

[10]. Suzuki M, et al. Role of sarcolemmal K(ATP) channels in cardioprotection against ischemia/reperfusion injury in mice. J Clin Invest 2002;109(4):509–16. 10.1172/JC114270. [PubMed: 11854323]

[11]. Sato T, et al. Selective pharmacological agents implicate mitochondrial but not sarcolemmal K(ATP) channels in ischemic cardioprotection. Circulation 2000;101(20):2418–23. [PubMed: 10821820]

[12]. Garlid KD, et al. Cardioprotective effect of diazoxide and its interaction with mitochondrial ATP-sensitive K+ channels. Possible mechanism of cardioprotection Circ Res 1997;81(6):1072–82. [PubMed: 9400389]

[13]. Ye B, et al. Molecular identification and functional characterization of a mitochondrial sulfonylurea receptor 2 splice variant generated by intraexonic splicing. Circ Res 2009;105(11):1083–93. 10.1161/CIRCRESAHA.109.195040. [PubMed: 19797704]

[14]. El-Meanawy SK, et al. Overexpression of a short sulfonylurea splice variant increases cardiac glucose uptake and uncouples mitochondria by regulating ROMK activity. Life (Basel) 2023;13(4). 10.3390/life13041015.

[15]. Dunlay SM, Roger VL. Gender differences in the pathophysiology, clinical presentation, and outcomes of ischemic heart failure. Curr Heart Fail Rep 2012;9(4):267–76. 10.1007/s11897-012-0107-7. [PubMed: 22864856]

[16]. Raparelli V, et al. Correction to: sex and gender differences in ischemic heart disease: endocrine vascular disease approach (EVA) study design. J Cardiovasc Transl Res 2020;13(1):26. 10.1007/s12265-019-09870-9. [PubMed: 30756360]

[17]. Wenger NK. Special issue on atherosclerotic cardiovascular disease: sex and gender differences. Atherosclerosis 2023:117271. 10.1016/j.atherosclerosis.2023.117271.

[18]. Lee CY, et al. Sex and gender differences in presentation, treatment and outcomes in acute coronary syndrome, a 10 year study from a multi-ethnic Asian population: the Malaysian National Cardiovascular Disease Database-Acute Coronary Syndrome (NCVD-ACS) registry. PLoS One 2021;16(2):e0246474. 10.1371/journal.pone.0246474. [PubMed: 33556136]

[19]. Connelly PJ, et al. The importance of gender to understand sex differences in cardiovascular disease. Can J Cardiol 2021;37(5):699–710. 10.1016/j.cjca.2021.02.005. [PubMed: 33592281]

[20]. Aggarwal NR, et al. Sex differences in ischemic heart disease: advances, obstacles, and next steps. Circ Cardiovasc Qual Outcomes 2018;11(2):e004437. 10.1161/CIRCOUTCOMES.117.004437. [PubMed: 29449443]

[21]. Gao J, et al. Disrupting KATP channels diminishes the estrogen-mediated protection in female mutant mice during ischemia-reperfusion. Clin Proteomics 2014;11(1):19. 10.1186/1559-0275-11-19. [PubMed: 24936167]

[22]. Ranki HJ, et al. Gender-specific difference in cardiac ATP-sensitive K(+) channels. J Am Coll Cardiol 2001;38(3):906–15. 10.1016/s0735-1097(01)01428-0. [PubMed: 11527652]

[23]. Ranki HJ, et al. Ageing is associated with a decrease in the number of sarcolemmal ATP-sensitive K+ channels in a gender-dependent manner. Mech Ageing Dev 2002;123(6):695–705. 10.1016/s0047-6374(01)00415-8. [PubMed: 11850031]

[24]. Jiang H, et al. Skewer: a fast and accurate adapter trimmer for next-generation sequencing paired-end reads. BMC Bioinform 2014;15:182. 10.1186/1471-2105-15-182.

[25]. Robinson MD, McCarthy DJ, Smyth GK. edgeR: a Bioconductor package for differential expression analysis of digital gene expression data. Bioinformatics 2010;26(1):139–40. 10.1093/bioinformatics/btp616. [PubMed: 19910308]

[26]. Dobin A, et al. STAR: ultrafast universal RNA-seq aligner. Bioinformatics 2013;29(1):15–21. 10.1093/bioinformatics/bts635. [PubMed: 23104886]

[27]. Li B, Dewey CN. RSEM: accurate transcript quantification from RNA-Seq data with or without a reference genome. BMC Bioinform 2011;12:323. 10.1186/1471-2105-12-323.

[28]. Wojtovich AP, et al. A novel mitochondrial K(ATP) channel assay. Circ Res 2010;106(7):1190–6. 10.1161/CIRCRESAHA.109.215400. [PubMed: 20185796]

[29]. Stoller D, et al. Mice lacking sulfonylurea receptor 2 (SUR2) ATP-sensitive potassium channels are resistant to acute cardiovascular stress. J Mol Cell Cardiol 2007;43(4):445–54. 10.1016/j.yjmcc.2007.07.058. [PubMed: 17765261]

[30]. Aggarwal NT, et al. The mitochondrial bioenergetic phenotype for protection from cardiac ischemia in SUR2 mutant mice. Am J Physiol Heart Circ Physiol 2010;299(6):H1884–90. 10.1152/ajpheart.00363.2010. [PubMed: 20935152]

[31]. Aggarwal NT, Shi NQ, Makielski JC. ATP-sensitive potassium currents from channels formed by Kir6 and a modified cardiac mitochondrial SUR2 variant. Channels (Austin) 2013;7(6):493–502. 10.4161/chan.26181. [PubMed: 24037327]

[32]. Huang Y, et al. Genetic discovery of ATP-sensitive K(+) channels in cardiovascular diseases. Circ Arrhythm Electrophysiol 2019;12(5):e007322. 10.1161/CIRCEP.119.007322. [PubMed: 31030551]

[33]. Cox MM, et al. Chronic neonatal Diazoxide therapy is not associated with adverse effects. Online J Biol Sci 2014;14(1):49–56. 10.3844/ojbsci.2014.49.56. [PubMed: 25587244]

[34]. Jovanovic A. Ageing, gender and cardiac sarcolemmal K(ATP) channels. J Pharm Pharmacol 2006;58(12):1585–9. 10.1211/jpp.58.12.0004. [PubMed: 17331321]

[35]. Walewska A, et al. Methods of measuring mitochondrial potassium channels: a critical assessment. Int J Mol Sci 2022;23(3). 10.3390/ijms23031210.

[36]. Kravenska Y, Checchetto V, Szabo I. Routes for potassium ions across mitochondrial membranes: a biophysical point of view with special focus on the ATP-sensitive K(+). Channel Biomol 2021;11(8). 10.3390/biom11081172.

[37]. Dong K, et al. An amino acid triplet in the NH2 terminus of rat ROMK1 determines interaction with SUR2B. J Biol Chem 2001;276(47):44347–53. 10.1074/jbc.M108072200. [PubMed: 11567030]

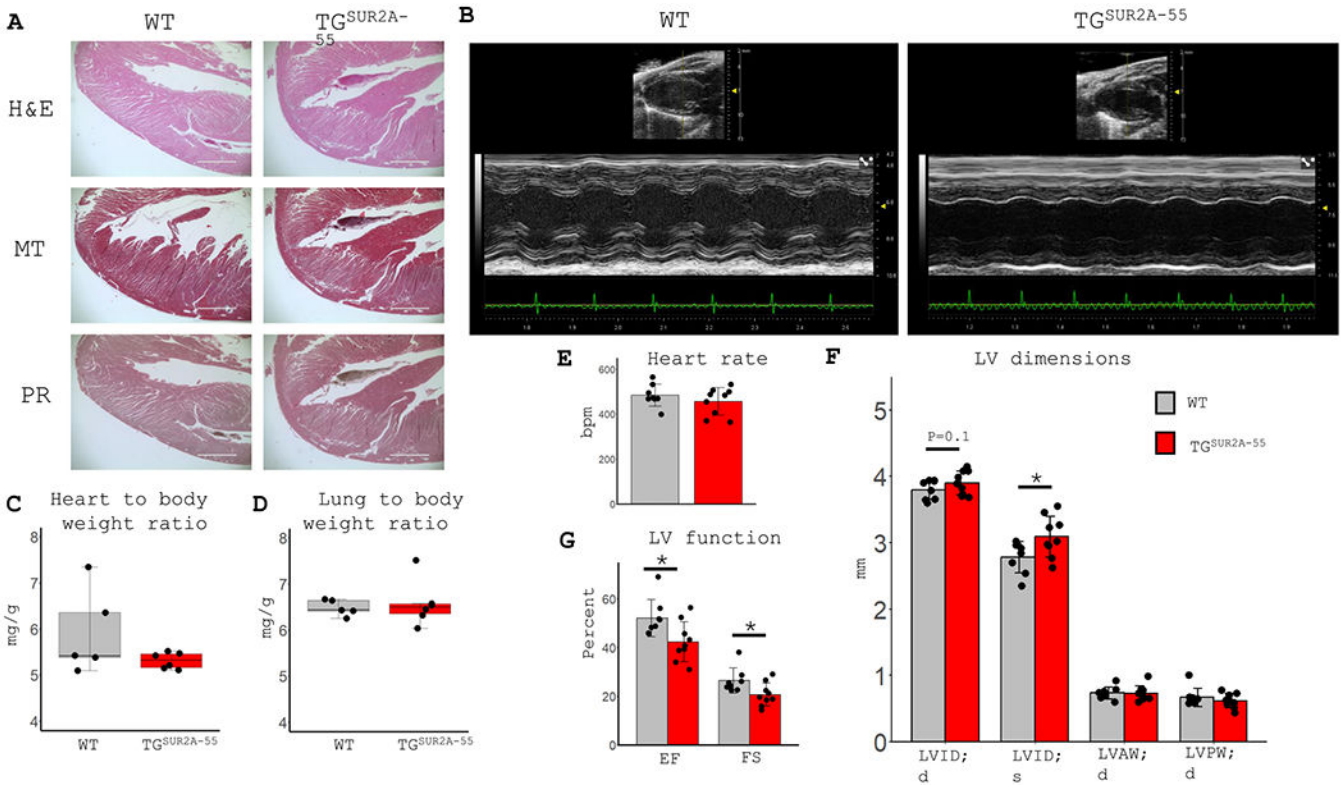

Fig. 1.

Histopathology and echocardiography from WT and TG$^{SUR2A-55}$ female mice. A) Histology B) Echocardiographic images C) Heart to Body ratio D) Lung to body weight ratio E) Heart rate F) Echocardiographic chamber dimensions G) Echocardiographic left ventricular function; ejection fraction and % fractional shortening. H&E, Hematoxylin Eosin; MT, Mason trichrome; PS, Picrosirius red; scale bar = 1000 μm; LVID;d, left ventricular end diastolic dimension; LVID;s, left ventricular end systolic dimension; LVAW; d, left ventricular anterior wall in diastole; LVPW;d, left ventricular posterior wall in diastole. N= 5 for WT and N=6 for TG$^{SUR2A-55}$ for gross pathology (C and D), N = 8 for WT and N=9 for TG$^{SUR2A-55}$ for echocardiography (E-G). Data are presented as boxplots or mean ± SD. Differences between groups were assessed using the student t-test, *$P < 0.05$.

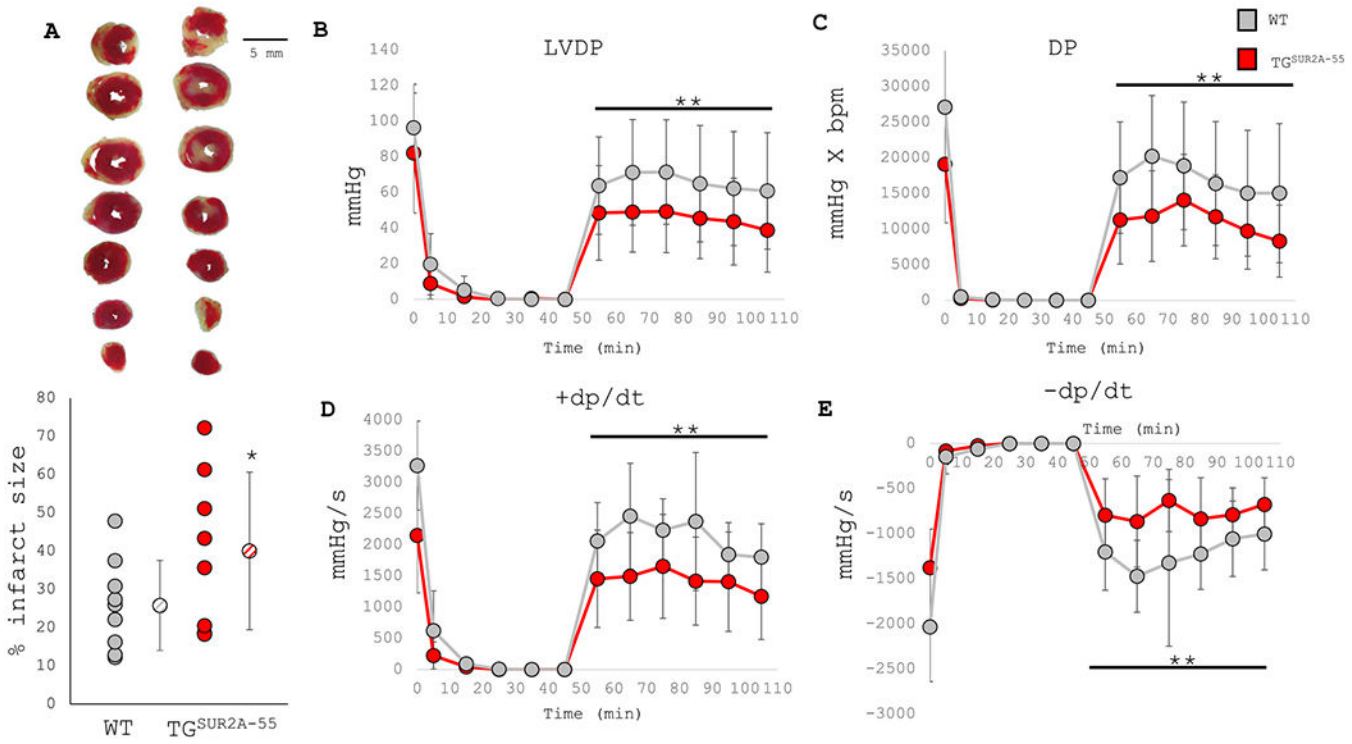

Fig. 2.

The effect of ischemia reperfusion injury on left ventricular function and infarct size in WT vs. TG$^{SUR2A-55}$ female mice. A) Representative sections after IR injury stained with TTC (top) and cumulative data (bottom). Hemodynamic recovery of function after IR injury, B) LVDP C) DP D) +dp/dt and E) −dp/dt. LVDP, left ventricular developed pressure; DP, double product; scale bar = 5 mm. N=9 for WT, N=8 for TG$^{SUR2A-55}$. Data are presented as mean ± SD, Differences between groups were assessed using student t-test for infarct size and two –way AVONA for hemodynamics. *$P < 0.05$; **$P < 0.001$.

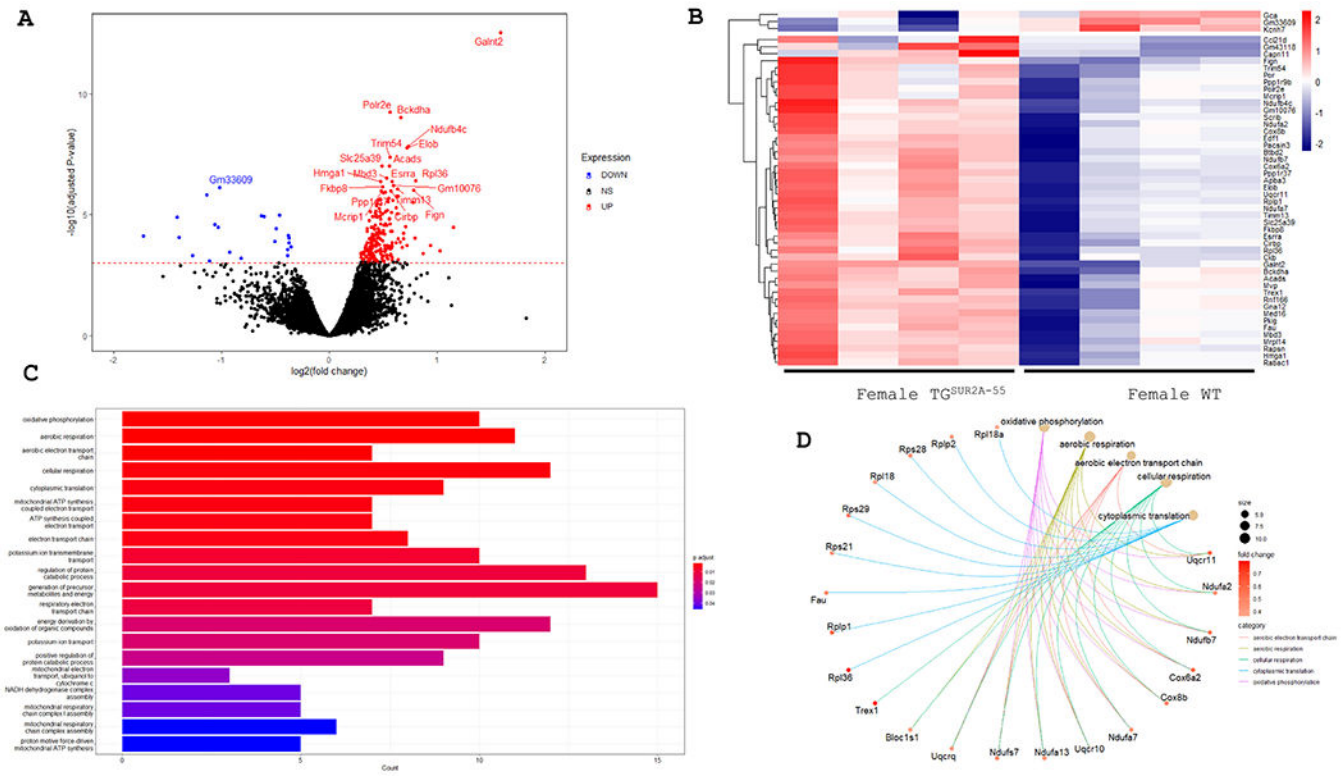

Fig. 3.

RNA-Seq analysis identifies differences in gene expression between hearts from female WT vs. TG$^{SUR2A-55}$ mice. A) Volcano plot of significantly differentially expressed genes showing distribution of significance [−log10(qvalue)] vs. fold change [log2(fold change)] for all genes (red, up-regulated; blue, down-regulated). B) Heatmap shows the top 50 significantly (FDR ≤0.05) differentially expressed genes in female mouse hearts between WT and TG$^{SUR2A-55}$. Each row of the heatmap represents the z-score values of one differentially expressed gene across all samples (blue, low expression; red, high expression). C) Gene ontology (GO) enrichment analysis showing the top significantly enriched GO terms of down-and upregulated DEGs in female WT compared to TG$^{SUR2A-55}$ mice hearts. The x-axis represents the number of DEGs involved in GO terms, and the y-axis the significantly enriched GO terms. D) Network diagram showing the relationship between the DEGs found in female WT compared to TG$^{SUR2A-55}$ mouse hearts and GO terms.

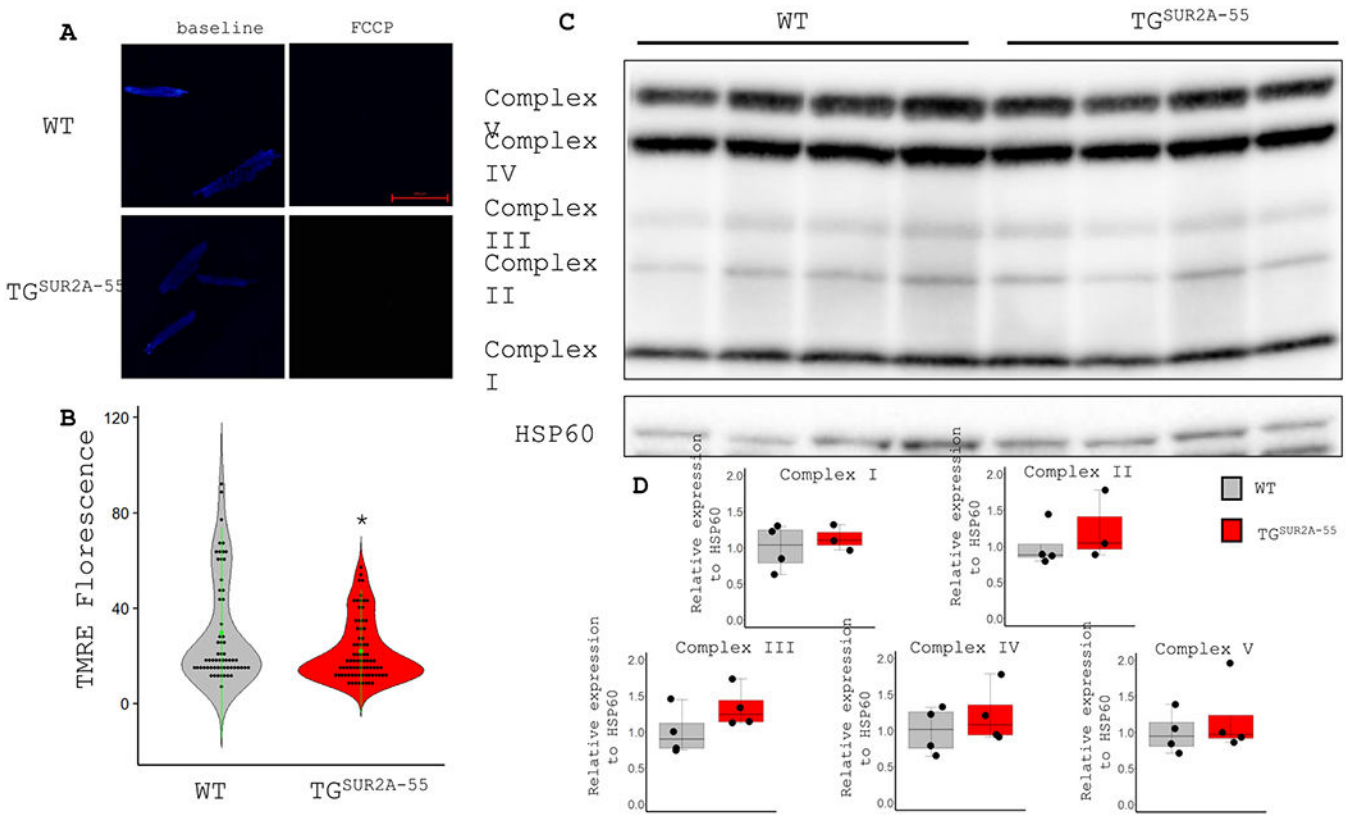

Fig. 4.

Mitochondrial membrane potential and ETC enzyme components in female WT and $TG^{SUR2A-55}$ mouse hearts. A) Confocal images of isolated adult mouse cardiomyocytes stained with TMRE at baseline and after FCCP treatment at 20× magnification. B) Cumulative data of TMRE fluorescence. C) Representative images of western blots D.) Quantification of bands illustrates similar cardiac mitochondrial protein expression between WT and $TG^{SUR2A–55}$. For TMRE experiments WT n=61 cells; $TG^{SUR2A-55}$ n=77cells from 3 experimental animals; scale bar = 100 μm; for western blots N=4. Data are presented as violin and box plots. Differences between groups were assessed using student t-test,* $P <$ 0.05.

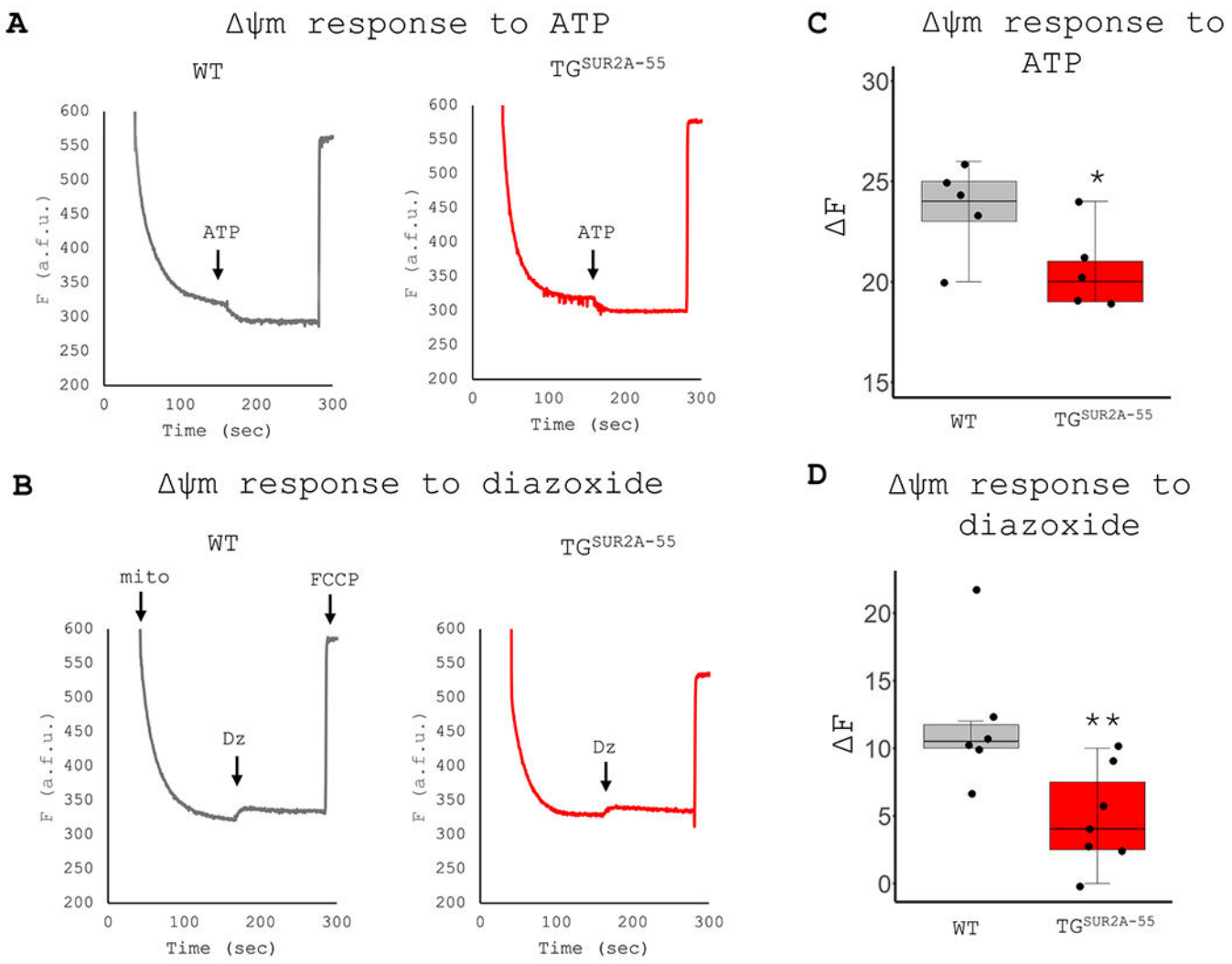

Fig. 5.

Response to diazoxide and ATP in isolated heart mitochondria from WT and TG$^{SUR2A-55}$ female mice. A and B) Representative traces of Δψm measured by rhodamine 123 fluorescence in isolated mitochondria from WT and TG$^{SUR2A–55}$ mouse hearts treated with ATP or diazoxide. C and D) Summary data of Δψm after ATP (1000 μm) or diazoxide (100 μm) treatment. The sample size of the experiments represents the total number of measurements made (N) for the number of mice used for each group (n). For $^{SUR2A-55}$, N,n = 6,7 for diazoxide and 6,5 for ATP. For WT, N,n = 6,6 for Diazoxide and 6,5 for ATP. Differences between groups were assessed using the student t-test, $^{**}P < 0.01$;$^{*}P < 0.05$.

Table 1

Baseline hemodynamic characteristics of isolated perfused hearts.

	WT	$TG^{SUR2A-55}$	P Value
LVDP (mmHg)	96.3 ± 8.1	82.1 ± 11.9	0.165
DP (mmHg•bpm)	27,097.9 ± 3510.2	19,096.1 ± 2912.1	0.052
+dp/dt (mmHg/s)	3269.0 ± 237.7	2148.6 ± 325.6	0.006*
−dp/dt (mmHg/s)	−2034.1 ± 142.9	−1377.5 ± 214.9	0.010*
HR (bpm)	239.0 ± 35.4	219.9 ± 30.9	0.073

LVDP, left ventricular developed pressure; DP, double product; +dp/dt, maximum pressure derivative; −dp/dt, minimum pressure derivative.